



Original Article

Synthesis of Nanoplatelet Zinc Borate and its Combination with Expandable Graphite and Red Phosphorus as Flame Retardants for Polypropylene

Truong Cong Doanh¹, Hac Thi Nhung^{2,3}, Nguyen Thi Hanh^{2,3},
Nguyen Thi Thu Hien², Doan Tien Dat², Vu Minh Tan¹, Hoang Mai Ha^{2,3*}

¹Hanoi University of Industry, 298 Cau Dien, Bac Tu Liem, Hanoi, Vietnam

²Institute of Chemistry, Vietnam Academy of Science and Technology,
18 Hoang Quoc Viet, Cau Giay, Hanoi, Vietnam

³Graduate University of Science and Technology, Vietnam Academy of Science and Technology,
18 Hoang Quoc Viet, Cau Giay, Hanoi, Vietnam

Received 08 November 2021

Revised 14 April 2022; Accepted 14 April 2022

Abstract: The zinc borate nanoparticles ($2\text{ZnO}\cdot 3\text{B}_2\text{O}_3\cdot 3\text{H}_2\text{O}$) were successfully prepared by precipitation reaction in aqueous solutions of borax and zinc sulfate using oleic acid as a surfactant. The structural, morphological characteristics and the wettability of the particle surface were studied through Fourier transform infrared spectroscopy (FT-IR), X-ray diffraction (XRD), scanning electron microscopy (SEM), and the contact angle. The hydrophobic zinc borate (n-ZB) had nanoplatelet morphology with a diameter of 1.0 - 1.5 μm and thickness of about 90 nm. Nano zinc borate showed a synergistic influence with expandable graphite (EG) and red phosphorus (RP) on the flame retardant properties and thermo-oxidative stability of polypropylene (PP). The nanocomposite 7n-ZB/7RP/7EG/PP achieved the V-1 UL94 verticle burning test with a limited oxygen index of 23.7% and the char yield of 14.67 wt.% at 900 °C. Furthermore, the fire retardant performance and the mechanical properties of the nanocomposites loading ZB nanoparticles were improved compared with the composites employing commercial ZB microparticles.

Keywords: Nanoplatelets, nano zinc borate, hydrophobic, flame retardant.

1. Introduction

Polypropylene (PP) is a synthetic polymer of great industrial importance, it is known to be

an extensively used material with a numerous range of applications in clothing, packaging, floor coverings, medical instruments, home appliances, automotive industry, wall coverings, etc [1, 2]. However, PP is a very combustible material, thus advancement in fire retardant performance is required to broaden its potential applications [3]. To improve the fire

* Corresponding author.

E-mail address: Hoangmaiha@ich.vast.vn

<https://doi.org/10.25073/2588-1140/vnunst.5402>

behavior of polymers, a large number of organic and inorganic flame retardant additives have been researched and developed [4-6]. The current trend of most research interest is to produce composite materials containing inorganic additive particles such as magnesium hydroxide, aluminum hydroxide, and zinc borates or intumescent flame retardant systems such as red phosphorus, expandable graphite [6-13]. This is because of their low-level toxicity, low fume, and no dioxin generation in the combustion process.

For inorganic mineral flame retardants, zinc borate is known to be a commonly used ingredient in both polymers loading halogen and halogen-free [14-17]. Zinc borate acts as a condensed phase flame retardant by endothermic dehydration, a char booster, a fire retardant synergist with many other additives, and a smoke suppressant. However, its drawbacks are a requirement of a large load to achieve a necessary level of flame retardancy for a composite and the poor compatibility of this inorganic material with polymer matrices, resulting in a significant decrease in the mechanical properties of composites and difficult processing. Some effective solutions can be applied to surmount this problem such as the change of the particle size and shape and the organic surface modification of the particle. Some studies on the preparation of nanostructured zinc borate have been reported. Three kinds of ZB ($2\text{ZnO}\cdot 3\text{B}_2\text{O}_3\cdot 7\text{H}_2\text{O}$, $2\text{ZnO}\cdot 3\text{B}_2\text{O}_3\cdot 3.5\text{H}_2\text{O}$, and $3\text{ZnO}\cdot 3\text{B}_2\text{O}_3\cdot 5\text{H}_2\text{O}$) were synthesized by the reaction between $\text{Zn}(\text{NO}_3)_2\cdot 6\text{H}_2\text{O}$, $\text{Na}_2\text{B}_4\text{O}_7\cdot 10\text{H}_2\text{O}$, and H_3BO_3 as the reactants at different conditions [18]. Ata and co-workers were also prepared nano ZB ($2\text{ZnO}\cdot 3\text{B}_2\text{O}_3\cdot 3.5\text{H}_2\text{O}$) via a liquid-solid reaction between ZnO and H_3BO_3 [19]. Gao et al synthesized a nanosphere like zinc borate $4\text{ZnO}\cdot \text{B}_2\text{O}_3\cdot \text{H}_2\text{O}$ through a homogeneous precipitation reaction [20]. However, reports of the impact of nano zinc borate on the fire resistance and the mechanical properties of polymers, especially the combination of the nanoparticles and other halogen-free additives have been relatively few.

In addition, red phosphorus (RP) is a relatively inexpensive and highly effective flame retardant. The flame resistance of RP manifests itself in both the condensed and gaseous phases through different mechanisms, which is suitable for a wide variety of polymers [9-11]. RP has been successfully applied to enhance the flame retardancy of many polymers including polyamides, polyethylenes, polyesters, polyolefins, etc [12-15]. Expandable graphite (EG) is another intumescent flame retardant that can expand into a large insulative char layer covering the surface of materials when heated, thereby providing fire retardant efficiency [16, 17].

In the scope of this study, we fabricated polyhedral nano zinc borate $2\text{ZnO}\cdot 3\text{B}_2\text{O}_3\cdot 3\text{H}_2\text{O}$ by employing oleic acid as a surfactant and characterized the structure, morphology, and hydrophobic property of the obtained nanoparticles. We also prepared flame retardant composites based on PP plastic using a combination of nano zinc borate obtained from the above synthesis and other halogen-free compounds such as RP and EG as flame retardant additives. The flame retardancy, thermo-oxidative stability, and the mechanical properties of the composite were studied via the UL94 vertical burning test, limited oxygen index, thermogravimetric analysis, and tension test.

2. Methodology

2.1. Materials

Zinc sulfate heptahydrate ($\text{ZnSO}_4\cdot 7\text{H}_2\text{O}$, 99%), borax decahydrate ($\text{Na}_2\text{B}_4\text{O}_7\cdot 10\text{H}_2\text{O}$, $\geq 99.5\%$), and oleic acid (technical grade, 90%) were supplied by Sigma, Germany; Absolute ethanol ($\geq 99.7\%$) was purchased from China. Commercial polypropylene with trademark of Advanced-PP 1102K (density = $0.91 \text{ g}\cdot \text{cm}^{-3}$, melt flow index ($230 \text{ }^\circ\text{C}$. 2.16 kg^{-1}) = $3.4 \text{ g}\cdot 10 \text{ min}^{-1}$) was provided by Advanced Petrochemical Company, Saudi; Commercial zinc borate (98.8%) and expandable graphite (+100 mesh, expansion rate = $280 \text{ mL}\cdot \text{g}^{-1}$) was a commercial product of China; Red

phosphorus ($\geq 97.0\%$) obtained from Sigma, Germany. All reagents had high purity and were used without any further treatment.

2.2. Sample Preparation

Synthesis of nano zinc borate

Nanostructured zinc borate was synthesized by a homogeneous precipitation reaction [21]. Two solutions consisting of 19.05 g $\text{Na}_2\text{B}_4\text{O}_7 \cdot 10\text{H}_2\text{O}$ in 100 mL DI water and 1.25 g oleic acid (OA) in 20 mL absolute ethanol were injected into a three-neck round-bottom flask capacity of 500 mL with a reflux condenser.

The system was stirred at a speed of 700 rpm and heated to 70 °C. 28.76 g of $\text{ZnSO}_4 \cdot 7\text{H}_2\text{O}$ was dissolved in 100 mL H_2O and the solution was then dropped into the mixture for about 30 min. After the addition was ended, the above mixture was continuously stirred at 70 °C for 6.5 hrs. Finally, the white precipitate was filtered and washed many times with ethanol and DI water to eliminate unreacted substances and by-products and dried at 80 °C for 12 hrs in the oven to obtain about 8.5 g nano zinc borate, approximately a reaction efficiency of 80%.

Table 1. Compositions of samples

Sample	PP (wt.%)	n-ZB (wt.%)	ZB (wt.%)	RP (wt.%)	EG (wt.%)
Neat PP	100	-	-	-	-
21n-ZB/PP	79	21	-	-	-
21ZB/PP	79	-	21	-	-
21RP/PP	79	-	-	21	-
21EG/PP	79	-	-	-	21
7ZB/7RP/7EG/PP	79	-	7	7	7
7n-ZB/7RP/7EG/PP	79	7	7	7	-

Preparation of flame retardant composites

First of all, PP resin and flame retardant additives were dried at 80 °C for 12 hrs to remove any moisture before being used in the preparation of composites. All samples were fabricated by melt mixing method with the detailed formulations of samples mentioned in Table 1. The mixtures of the polymer and additives were loaded into the chamber of the Haake mixer and extruder system (USA) and blended at 175 °C with a rotation speed of 50 rpm. Under the rotation of the rotor and the heat supplied to the mixing chamber, the ingredients are mixed and turned into a viscous flow. After 8 minutes of mixing, the molten mixture was removed from the mixing chamber and quickly flattened on a Toyoseiky hydraulic machine (Japan) at 200 °C for 4 minutes, with a

force of 10 - 12 MPa, and then the samples were allowed to cool naturally. Finally, the samples were prepared according to standard dimensions of measurements and characterizations.

2.3. Characterization

Fourier-transform infrared spectroscopy: FT-IR spectrum of nano zinc borate was obtained on a Spectrum Two FTIR spectrometer (PerkinElmer, USA) in the wavenumber range of 4000 - 450 cm^{-1} at room temperature.

X-ray diffraction: XRD pattern of nano zinc borate was recorded on the D8 Advance system (Bruker, USA) over the 2θ range from 10° to 70° employing $\text{Cu K}\alpha$ radiation with $\lambda = 0.15406 \text{ nm}$ at 45 kV and 40 mA.

Field Emission Scanning electron microscope (FE-SEM): the morphology of nano zinc borate and composites were observed on an S-4800 instrument (Hitachi, Japan) under a voltage range of 2 - 5 kV at room temperature.

The water contact angle: the wettability of zinc borate powders with and without OA was measured on a goniometer employing 5 μ L water droplets deposited on the surface of samples by a microsyringe. Contact angle value (CA) was obtained by taking a static picture of the liquid-air interface and was analyzed by ImageJ software. The result was an average value of three measurements at different areas of a sample.

The Vertical Burning Test (UL94-V): This test is applied in accordance with the ASTM D 3801-96 standard on a horizontal and verticle flame chamber. Test specimens were prepared on bars with dimensions of 125 x 13 x 3 mm. The flame retardancy of materials was classified according to UL94-V into three levels consisting of V-0 (best fire resistance), V-1 (good fire resistance), and V-2 (medium fire resistance).

Limited oxygen index (LOI) test: LOI values of neat PP and its composites were measured by an oxygen index apparatus (Yasuda 214, Japan). Tests were conducted on bars with dimensions of 125 \times 13 \times 3 mm according to ASTM D 2863-97.

Thermogravimetric analysis (TGA): TGA data of neat PP and the composite were obtained on a LABSYS Evo STA analyzer (Setaram, UK). The tests were carried out with around 10 mg of samples with a heating speed of 10 $^{\circ}$ C. min^{-1} from room temperature to 900 $^{\circ}$ C.

The tensile strength and the elongation at the break of the materials were conducted following the ASTM D638 standard on the GOTECH AI-7000M machine (Taiwan). These tests were carried out with a tensile rate of 50 mm. min^{-1} . The obtained data of each formulation is the average value of 3 measurements.

3. Results and Discussion

3.1. Structure and Morphology of Nano Zinc Borate

Fig. 1 illustrates the FT-IR spectrum and the XRD pattern of the synthesized nano zinc

borate. As shown from the spectrum, the absorption peak at 3380 cm^{-1} is assigned to the stretching vibrations of the O-H bond. The diffraction peak at 1628 cm^{-1} is attributed to the bending vibrations of the H-O-H bond, which exhibits that the synthesized compound includes water crystals. The absorption peak at 1129 cm^{-1} is because of the B₍₃₎-O stretching vibrations and 654 cm^{-1} is corresponding to the B₍₃₎-O bending vibrations in-plane. The peaks at 1027 and 965 cm^{-1} can be ascribed to the B₍₄₎-O asymmetric stretching and the B₍₄₎-O symmetric stretching, respectively. The peak at 510 cm^{-1} can be due to the M-O bond in which M is metal ions [22-24]. These vibrations characterize the bonds in the zinc borate compound. In addition, the absorption peaks at 2925 cm^{-1} , 2853 cm^{-1} , and 1550 cm^{-1} have been assigned to the asymmetric and symmetric stretching vibrations of -CH, and the -COO symmetric stretching in the carboxylate groups of oleic acid, respectively [25], which indicates that the surfactant is adsorbed on the particle surface. On the other hand, the sharp diffraction peaks of the product are displayed in the XRD pattern (Fig. 1b), which expresses the compound has high crystallinity. All peaks are in good agreement with data of 2ZnO.3B₂O₃.3H₂O which has No. 21-1473 in the JCPDS file and previous reports [21]. No characteristic peaks of other compounds such as unreacted substances or other by-products are observed, which reveals that the obtained product has high purity. Therefore, the results manifest that the synthesized particle is 2ZnO.3B₂O₃.3H₂O crystalline phases.

The morphologies of synthesized zinc borate particles without and with the presence of the OA surfactant are shown in Fig. 2 (a,b). In general, these particles obtain polyhedral shape zinc borates. However, it may be seen that the particle size of ZB without OA is not uniform with a large diameter range from 0.5 μm to 2.5 μm (Fig. 2a). In contrast, ZB synthesized in the presence of OA is nanoplatelets and their morphology is relatively consistent with a diameter of about 1.0 - 1.5 μm and a thickness of approximately 90 nm (Fig. 2b).

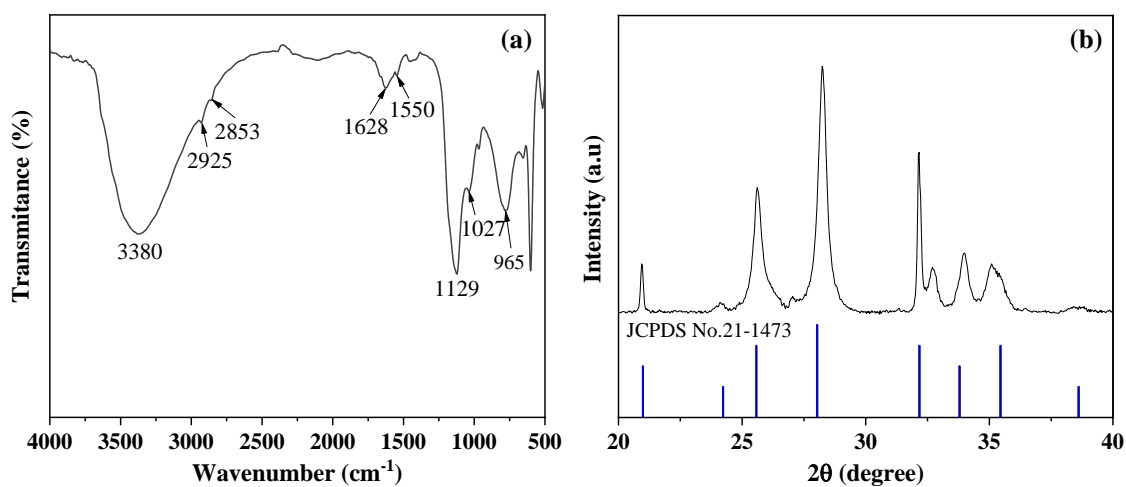


Figure 1. FT-IR spectrum (a) and XRD pattern (b) of nano $Zn_2B_6O_{11} \cdot 3H_2O$.

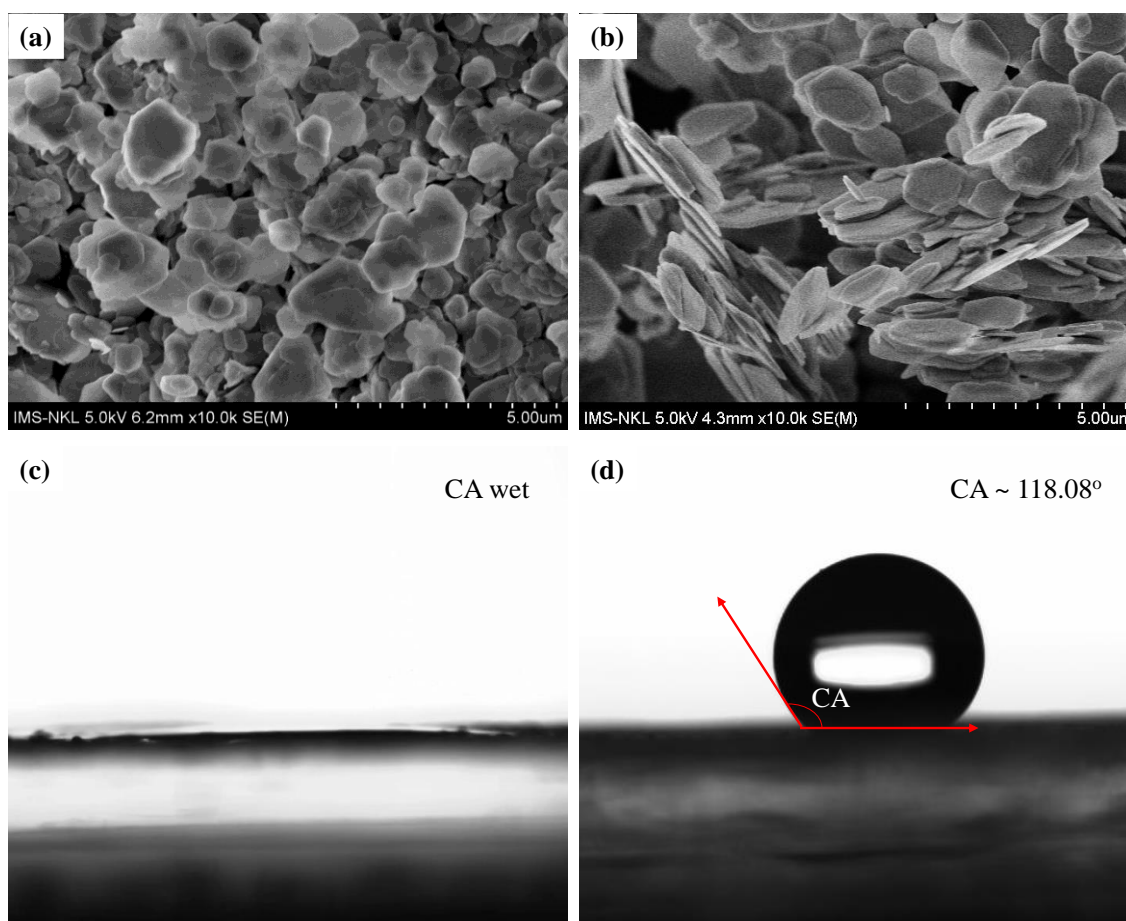


Figure 2. SEM images of zinc borate particles without (a) and with (b) oleic acid, and water droplet contact angle images on the surface of these powders (c, d), respectively.

The morphology of ZB transforms from irregular to regular, this verifies the effectiveness of the OA surfactant on the modulation of the shape of the particles.

To measure the hydrophobicity property of nanoparticle surfaces, the water contact angle index is commonly used. Fig. 3 (c,d) exhibits the contact angle images of water droplets on the surface of the ZB samples synthesized without and with oleic acid.

As shown in Fig. 3c, the water droplet is rapidly absorbed when it is dropped on the

surface of the pure zinc borate powder with a contact angle value of approximately 0°. This result displays that the product is a superhydrophilic material, resulting in poor dispersion of the material in the organo-matrix. However, with the presence of OA, the shape of the water droplet placed on the ZB surface is spherical with a considerable growth in the contact angle value to about 118.08°, which reveals the surface of ZB transfers from superhydrophilic to hydrophobic [26].

Table 2. The results of the UL94-V, LOI, and tension tests of samples

Sample	UL94-V rating	LOI value (%)	Tensile strength (MPa)	Elongation (%)
Neat PP	No rating	16.8	25.84 ± 0.6	62.93 ± 8.0
21ZB/PP	No rating	19.3	24.67 ± 0.2	40.49 ± 5.0
21RP/PP	No rating	21.1	23.55 ± 0.5	38.18 ± 6.0
21EG/PP	No rating	20.2	22.02 ± 1.0	19.07 ± 5.0
21n-ZB/PP	No rating	19.7	25.17 ± 0.2	58.85 ± 4.0
7ZB/7RP/7EG/PP	V-1	23.2	23.69 ± 0.7	30.17 ± 6.0
7n-ZB/7RP/7EG/PP	V-1	23.7	24.62 ± 0.4	35.12 ± 5.0

3.2. Fire Retardant Performance

Fire behavior of neat PP and the composites were examined through the UL94 and LOI tests, the results are presented in Table 2. From these data, it demonstrated that neat PP is highly flammable with a quite low LOI of 16.8%. The fire-retardant properties of the polymer are improved upon the addition of the fillers such as ZB, EG, and RP. Particularly, the LOI value of PP increases from 16.8% to 19.3%, 20.2%, and 21.1% when adding 21 wt.% ZB, EG, and RP into the PP matrix, respectively. However, the composites 21ZB/PP, 21RP/PP, and 21EG/PP do not achieve any level in the UL94-V rating. It is obvious that the flame retardancy of the composite loading all three components is

significantly enhanced compared to the composites containing only one filler at the same total content of additives. The 7ZB/7RP/7EG/PP composite reaches the UL94-V1 rating with a considerable increase in the LOI value to 23.2%. The explanation for the result is the synergistic influence of three flame retardant mechanisms of the additives to protect the composite. Phosphoric oxide from the oxidation of RP could react with water to form a film layer of some types of phosphoric acid covering the surface of the material in the combustion, thereby improving the fire performance of the composite [27, 28]. The water released from the dehydration of ZB can accelerate the conversion of these acid layers from RP. Furthermore, the degradation of zinc borate can produce a glass layer on the char

surface which can reinforce the char structure of the composite. For EG, at around 200 °C, carbon layers of EG react with H₂SO₄ (an intercalated compound between the layers of graphite) and form blown gases such as CO₂, SO₂ which make the carbon layers separate from each other. Consequently, an insulative massive char layer with a multiple of its initial size is generated on the burnt surface of the material, therefore supplying a great fire retardant performance for the composite [29]. Expandable graphite is an effective flame retardant for thermosetting resins [29-31]. However, the melting property of thermoplastics causes the instability of the char layer from EG on the surface of the polymers, thus the flame retardant performance of EG is lower in these polymers. The combination of ZB, RP, and EG makes the structure of the char layer of the composite more stable and decreases the dripping phenomenon of the polymer, resulting in the high flame retardant effect of EG in the thermoplastic. The results indicate the synergistic effect of three additives on the fire retardant enhancement of the PP

composite. The effect of nano zinc borate on improving the fire behavior of PP was also studied. The result shows that the flame retardancy of the composite loading nano ZB is higher than that of the composite containing commercial ZB microparticles at the same content. As shown in Table 2, the LOI value of the composites 21ZB/PP and 7ZB/7RP/7EG/PP rises from 19.3% and 23.2% to 19.7% and 23.7%, respectively, when replacing ZB microparticles with ZB nanoparticles at the same content. This increase could be explained by the better dispersion of n-ZB in the polymer substrate.

3.3. Thermal Stability

The thermo-oxidative decomposition of PP and the nanocomposite 7n-ZB/7RP/7EG/PP was analyzed by the TGA method in air. Fig. 3 illustrates the TG and derivative thermogravimetric (dTG) curves of PP and the nanocomposite. The particular data which includes the temperature at 5 wt.% weight loss ($T_{5\%}$), the temperature at a maximum weight loss (T_{max}) and the char yield at 900 °C are listed in Table 3.

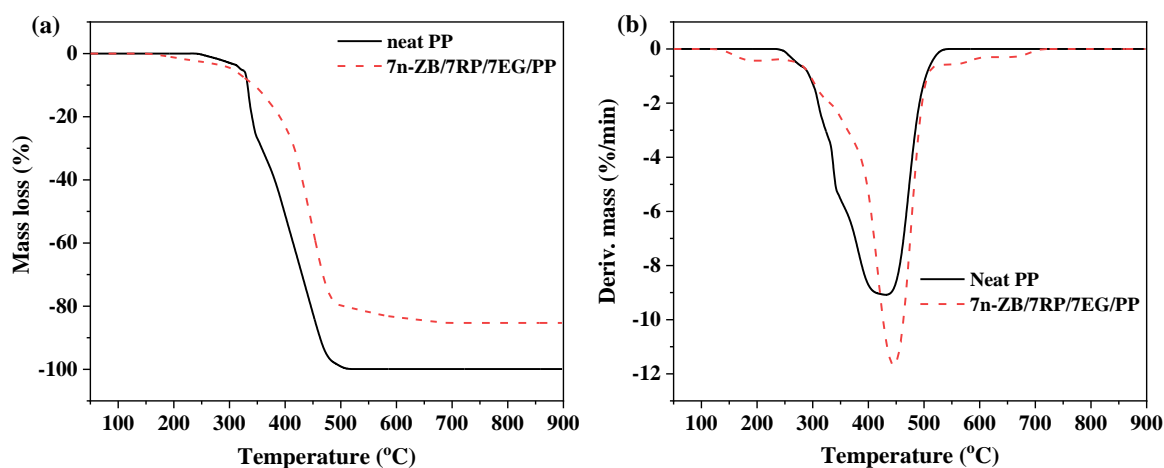


Figure 3. TG (a) and dTG curves (b) of pure PP and the nanocomposite in air.

Table 3. TGA data of pure PP and the nanocomposite in air

Sample	$T_{5\%}$ (°C)	T_{max} (°C)	Residue at 900 °C (wt.%)
Neat PP	320.6	431.9	0.1
7n-ZB/7RP/7EG/PP	296.5	445.7	14.67

Neat PP undergoes a single decomposition process. The polymer is degraded completely at 510 °C with $T_{5\%}$ of 320.6 °C, T_{max} of 431.9 °C, and a char residue of only 0.1% at 900 °C. The $T_{5\%}$ value of the nanocomposite is shifted to a lower temperature compared to the original PP corresponding to the early dehydration of nano zinc borate at approximately 180 °C [32]. However, the T_{max} value of the nanocomposite remarkably increases to 445.7 °C. Additionally, the residue of this nanocomposite at 900 °C is much higher than that of the original PP, about 14.67%. These results can be owing to the formation of the insulating barricade from the flame retardants limiting the heat transfer into the internal nanocomposite, resulting in a decline decomposition rate of the material. Therefore, it can conclude that the thermo-stability of PP is notably enhanced by the combination of all three fillers nano ZB, RP, and EG.

3.4. Mechanical Properties

The tensile strength and elongation values at the break of neat PP and the composites are detailed in Table 2 and Fig. 4. In general, these mechanical properties of PP degraded with the addition of the fillers, and EG causes the largest decrease among the three commercial additives. Specifically, the tensile strength and the elongation of the PP matrix reduce by 14.78% and 71.70%, respectively upon adding 21 wt.% EG. To explain this trend, the surface morphology of the composites was observed by SEM images and they are exhibited in Fig. 5. The declines of the composite loading microparticles are attributed to the poor interaction between the inorganic microparticles with the organic substrate and their large particle size, especially EG, which create defects in the composite and gaps between the additive and the organic matrix which can be observed in Fig. 5 (a-c), and

consequently interrupt the migration of macromolecule chains [33].

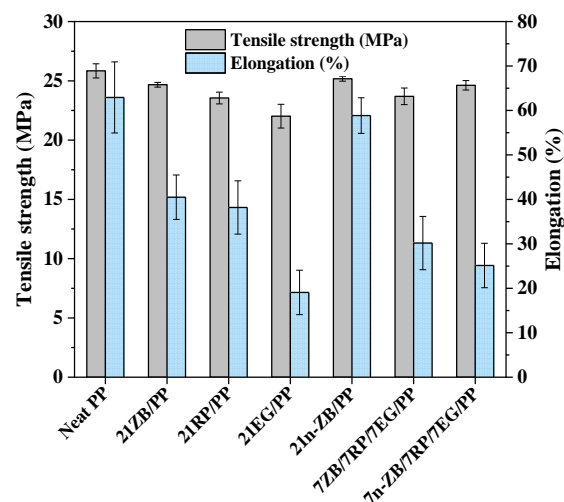


Figure 4. The results of the tension test of samples.

In addition, the effect of commercial and nano zinc borate on tensile properties was also studied. Compared with pure PP, the tensile stress and the tensile strain at break of nanocomposites 21n-ZB/PP minimally fall by 0.67 MPa and 4.08%, respectively. Moreover, the replacement of ZB microparticles in the composite containing all three fillers by nano ZB improves the mechanical properties of the composite. The tensile strength and the elongation of the composite 7ZB/7RP/7EG/PP climb to 24.62 MPa and 35.12%, respectively, when 7 wt.% the synthesized nano ZB substitutes for commercial ZB in this composite. The main reasons for the improvement are the smaller size of the ZB nanoparticles and their hydrophobic surface leading to an increase in the compatibility between the material and the polymer. As a result, the dispersion ability of nano ZB becomes better in the polymer matrix. In comparison with the composite containing micro ZB, it can be seen that the surfaces of the composites containing nano ZB become smoother without bulky agglomeration (Fig. 5).

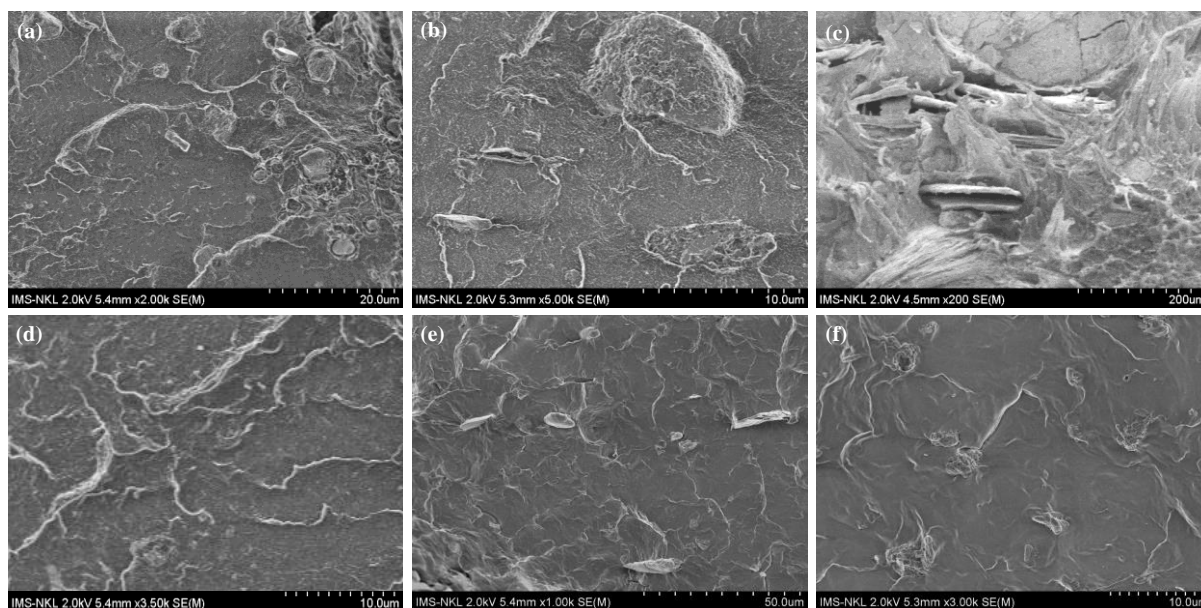


Figure 5. SEM images of composites 21ZB/PP (a), 21RP/PP (b), 21EG/PP (c), 21n-ZB/PP (d), 7ZB/7RP/7EG/PP (e), and 7n-ZB/7RP/7EG/PP (f).

4. Conclusion

In this work, nanoplatelet ZB with the molecular formula $2\text{ZnO} \cdot 3\text{B}_2\text{O}_3 \cdot 3\text{H}_2\text{O}$ was successfully synthesized by the homogeneous precipitation method. By analyzing morphology, we found that the size of synthesized nano zinc borate was uniform with a particle size of about 1.0 - 1.5 μm and thickness of roughly 90 nm. The contact angle tests with water droplets displayed that the OA surfactant changed the surface of zinc borate from superhydrophilic to hydrophobic with the increase of the CA value to 118.08°. The combination of zinc borate nanoparticles and RP and EG brought the synergistic effect on the fire resistance and thermal stability of PP. Furthermore, the tensile stress and the tensile strain at the break of the composites containing ZB nanoparticles improved compared to the figure of the composite loading commercial ZB microparticles.

Acknowledgments

This research was funded by the Vietnam Academy of Science and Technology under

grant number TĐPCCC.04/21-23. Particularly, Hac Thi Nhung acknowledges the financial support by the Institute of Chemistry under grant number VHH.2021.05.

References

- [1] S. Zhang, A. R. Horrocks, A Review of Flame Retardant Polypropylene Fibers, *Prog. Polym. Sci.*, Vol. 28, 2003, pp. 1517-1538.
- [2] G. Gleixner, Flame Retardant PP Fibres-lateat Developments, *Chem Fibers Int*, Vol. 51, 2001, pp. 422-434.
- [3] Z. Zhang, Z. Han, Y. Pan, D. Li, D. Wang, R. Yang, Dry Synthesis of Mesoporous Nanosheet Assembly Constructed by Cyclomatrix Polyphosphazene Frameworks and its Application in Flame Retardant Polypropylene, *Chem, Eng. J.*, Vol. 395, 2020, pp. 125076.
- [4] F. Qi, M. Tang, N. Wang, N. Liu, X. Chen, Z. Zhang, K. Zhang, X. Lu, Efficient Organic-inorganic Intumescent Interfacial Flame Retardants to Prepare Flame Retarded Polypropylene with Excellent Performance, *The Royal Society of Chemistry*, Vol. 7, 2017, pp. 31696-31706.
- [5] B. Xu, X. Wu, W. Ma, L. Qian, F. Xin, Y. Qiu, Synthesis and Characterization of a Novel

- Organic-inorganic Hybrid Char-forming Agent and its Flame-retardant Application in Polypropylene Composites, *J. Anal, Appl, Pyrolysis*, Vol. 134, 2018, pp. 231-242.
- [6] W. Wang, P. Wen, J. Zhan, N. Hong, W. Cai, Z. Gui, Y. Hua, Synthesis of a Novel Charring Agent Containing Pentaerythritol and Triazine Structure and its Intumescent Flame Retardant Performance for Polypropylene, *Polym, Degrad, Stab*, Vol. 144, 2017, pp. 454-463.
- [7] X. Chen, J. Yu, S. Guo, Structure and Properties of Polypropylene Composites Filled with Magnesium Hydroxide, *J. Appl, Polym, Sci.*, Vol. 102, 2006, pp. 4943-4951.
- [8] M. E. Üreyen, E. Kaynak, Effect of Zinc Borate on Flammability of PET Woven Fabrics, *Advances in Polymer Technology*, Hindawi, 2019, <https://doi.org/10.1155/2019/7150736>.
- [9] F. Laoutid, L. Bonnaud, M. Alexandre, J. M. L. Cuesta, Ph. Dubois, New Prospects in Flame Retardant Polymer Materials: From Fundamentals to Nanocomposites, *Mater Sci Eng R*, Vol. 63, 2009, pp. 100-125, <https://doi.org/10.1016/j.mser.2008.09.002>.
- [10] U. Braun, B. Scharrel, Flame Retardant Mechanisms of Red Phosphorus and Magnesium Hydroxide in High Impact Polystyrene, *Macromol Chem Phys*, Vol. 205, 2004, pp. 2185-2196, <https://doi.org/10.1002/macp.200400255>.
- [11] M. A. Fichera, U. Braun, B. Scharrel, H. Sturm, U. Knoll, C Jager, Solid-state NMR Investigations of Pyrolysis and Thermo-oxidative Decomposition Products of a Polystyrene/red Phosphorus/magnesium Hydroxide System, *J. Anal, Appl, Pyrolysis*, Vol. 78, 2007, pp. 378-386, <https://doi.org/10.1016/j.jaap.2006.09.013>.
- [12] L. A. Savas, M. Dogan, Flame Retardant Effect of Zinc Borate in Polyamide 6 Containing Aluminum Hypophosphite, *Polym, Degrad, Stab*, Vol. 165, 2019, pp. 101-109, <https://doi.org/10.1016/j.polymdegradstab.2019.05.005>.
- [13] Y. Xu, M. Tang, X. Chen, M. Chen, J. Yu, Y. Ma, Z. Sun, Z. Zhang, J. Lv, Effect of Red Phosphorus Masterbatch on Flame Retardancy and Thermal Stability of Polypropylene/thermoplastic Polyurethane Blends, *Polym, Polym, Compos*, Vol. 23, No. 2, 2015.
- [14] J. L. Zhuo, J. Dong, C. M. Jiao, X. L. Chen, Synergistic Effects between Red Phosphorus and Alumina Trihydrate in Flame Retardant Silicone Rubber Composites, *Plast, Rubber Compos*, Vol. 42, No. 6, 2013, pp. 239-243.
- [15] E. Gibertini, F. Carosio, K. Aykanat, A. Accogli, G. Panzeri, L. Magagnin, Silica-encapsulate Red Phosphorus for Flame Retardant Treatment on Textile, *Surf, Interfaces*, Vol. 25, 2021, <https://doi.org/10.1016/j.surfin.2021.101252>.
- [16] Z. Sun, Y. Ma, Y. Xu, X. Chen, M. Chen, J. Yu, S. Hu, Z. Zhang, Effect of the Particle Size of Expandable Graphite on the Thermal Stability, Flammability, and Mechanical Properties of High-Density Polyethylene/Ethylene Vinyl-Acetate/Expandable Graphite Composites, *Polym, Eng, Sci.*, 2014, pp. 1163-1169.
- [17] Z. Zheng, Y. Liu, L. Zhang, H. Wang, Synergistic Effect of Expandable Graphite and Intumescent Flame Retardants on the Flame Retardancy and Thermal Stability of Polypropylene, *J. Mater Sci*, Vol. 51, 2016, pp. 5857-5871.
- [18] Y. Cui, X. Liu, Y. Tian, N. Ding, Z. Wang, Controllable Synthesis of Three Kinds of Zinc Borates and Flame Retardant Properties in Polyurethane Foam, *Colloids and Surfaces A: Physicochem, Eng, Aspects*, Vol. 414, 2012, pp. 274-280, <http://doi:10.1016/j.colsurfa.2012.08.028>.
- [19] O. N. Ata, E. Şayan, B. Engin, Optimization and Modeling of Zinc Borate ($2\text{ZnO}\cdot 3\text{B}_2\text{O}_3\cdot 3.5\text{H}_2\text{O}$) Production with the Reaction of Boric Acid and Zinc Oxide, *J. Ind Eng Chem*, Vol. 17, 2011, pp. 493-497, <http://doi:10.1016/j.jiec.2010.09.018>.
- [20] P. Gao, W. Song, F. Ding, X. Wang, M. Li, Controllable Synthesis and Flame-retardant Properties of Spherical Zinc Borate Nanostructure, *Micro and Nano Letters*, Vol. 7, 2021, pp. 863-866, <http://doi:10.1049/mnl.2012.0418>.
- [21] Y. Tian, Y. He, L. Yu, Y. Deng, Y. Zheng, F. Sun, Z. Liu, Z. Wang, In Situ and One-step Synthesis of Hydrophobic Zinc Borate Nanoplatelets, *Colloids and Surfaces A: Physicochem, Eng*, Vol. 312, 2008, pp. 99-103.
- [22] T. Yumei, G. Yupeng, J. Man, S. Ye, H. Bala, Synthesis of Hydrophobic Zinc Borate Nanodiscs for Lubrication, *Materials Letters*, Vol. 60, 2006, pp. 2511-2515, <https://doi.org/10.1016/j.matlet.2006.01.108>.
- [23] L. Jun, X. Shuping, G. Shiyang, FT-IR and Raman Spectroscopic Study of Hydrated Borates, *Spectrochim, Acta*, Vol. 51, 1995, pp. 519-532, [https://doi.org/10.1016/0584-8539\(94\)00183-C](https://doi.org/10.1016/0584-8539(94)00183-C).
- [24] L. Zhihong, H. Mancheng, Synthesis, Characterization and Thermochemistry of a New Form of $2\text{MgO}\cdot 3\text{B}_2\text{O}_3\cdot 17\text{H}_2\text{O}$, *Thermochim, Acta*, Vol. 414, 2004, pp. 215-218, <https://doi.org/10.1016/j.tca.2003.12.026>.

- [25] J. Ibarra, J. Melendres, M. Almada, M. G. Burboa, P. Taboada, J. Juárez, M. A. Valdez, Synthesis and Characterization of Magnetite/PLGA/chitosan Nanoparticles, *Mater, Res, Express*, Vol. 2, 2015, pp. 095010, <https://doi.org/10.1088/2053-1591/2/9/095010>.
- [26] A. K. Kota, G. Kwon, A. Tuteja, The Design and Applications of Superomniphobic Surfaces, *NPG Asia Materials*, 2014, <https://doi.org/10.1038/am.2014.34>.
- [27] H. T. Nhung, N. T. Nhan, H. T. Oanh, N. T. T. Trang, D. Q. Tham, N. T. Ha, N. V. Tuyen, H. M. Ha, Synergistic Effects of Aluminum Hydroxide, Red Phosphorus, and Expandable Graphite on the Flame Retardancy and Thermal Stability of Polyethylene, *J. Appl, Polym, Sci*, 2020, <https://doi.org/10.1002/app.50317>.
- [28] G. Si, D. Li, Y. You, X. Hu, Investigation of the Influence of Red Phosphorus, Expansible Graphite and Zinc Borate on Flame Retardancy and Wear Performance of Glass Fiber Reinforced PA6 Composites, *Polymer Composites*, Vol. 38, No. 10, 2015, pp. 2090-2097, <https://doi.org/10.1002/pc.23781>.
- [29] M. Thirumal, D. Khastgir, N. K. Singha, B. S. Manjunath, Y. P. Naik, Effect of Expandable Graphite on the Properties of Intumescent Flame-retardant Polyurethane Foam, *J. Appl Polym Sci*, Vol. 110, 2008, pp. 2586-2594, <https://doi.org/10.1002/app.28763>.
- [30] M. Modesti, A. Lorenzetti, F. Simioni, G. Camino, Expandable Graphite as an Intumescent Flame Retardant in Polyisocyanurate-Polyurethane Foams, *Polym Degrad Stab*, Vol. 77, 2002, pp. 195-202, [https://doi.org/10.1016/S0141-3910\(02\)00034-4](https://doi.org/10.1016/S0141-3910(02)00034-4).
- [31] H. T. Nhung, P. D. Linh, N. T. Hanh, H. T. Oanh, D. T. H. Yen, N. T. Nhan, N. D. Tuyen, P. D. Long, T. T. Ha, N. T. H, N. T. Tung, H. M. Ha Influence of Organoclay on the Flame Retardancy and Thermal Insulation Property of Expandable Graphite/Polyurethane Foam, *J. Chem.*, Vol. 2019, pp. 1-8, <https://doi.org/10.1155/2019/4794106>.
- [32] S. Li, B. Long, Zi. Wang, Y. Tian, Y. Zheng, Q. Zhang, Synthesis of Hydrophobic Zinc Borate Nanoflakes and Its Effect on Flame Retardant Properties of Polyethylene, *J. Solid State Chem.*, Vol. 183, 2010, pp. 957-962.
- [33] Moustafa M. Y. Zaghoul, Mai M. Y. Zaghoul, Influence of Flame Retardant Magnesium Hydroxide on the Mechanical Properties of High Density Polyethylene Composites, *J. Reinf, Plast, Compos.*, Vol. 36, 2017, pp. 1-15, <http://doi:10.1177/0731684417727143>.